THEORETICAL STUDY OF RAMPING IN A STORAGE RING CONTAINING SUPERCONDUCTING MAGNETS WITH IRON

B. Krevet, H.O. Moser

Kernforschungszentrum Karlsruhe, Institut für Mikrostrukturtechnik,
Postfach 3640, D-7500 Karlsruhe 1, Germany

Abstract: Magnetic field calculations for a superconducting bending magnet with an iron shield and nonisomagnetic 3rd order symplectic tracking show that the dynamic aperture is adequate during ramping and can even be improved by the iron shield.

Introduction

Most of the superconducting bending magnets built or designed so far for accelerator applications employ iron surrounding the coils in order to increase the field in the beam region and to shield the outside space from the field. The relative contribution of the iron to the flux depends on the field strength. When the magnetic field is ramped the relative contributions from both iron and coils vary causing the nonlinear field content to change. This may give rise to a variation in the dynamic aperture.

There are several storage rings with superconducting bending magnets containing iron which have been successfully ramped[1]. However, different magnet designs need to be studied individually. In this work, the ramping behaviour of the superconducting bending magnet designed for the conceptual study of a synchrotron radiation source at Karlsruhe[2] (Fig.1) is investigated numerically. The magnetic field and the dynamic aperture are calculated for the field values of 0.4, 1.0, and 4.0 T. Time-dependent effects are not taken into account.

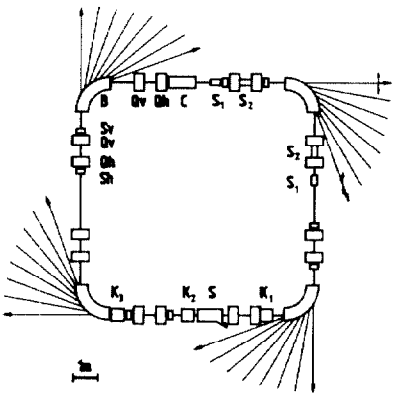

Fig. 1: Schematic layout of a general-purpose compact synchrotron radiation source as studied at Karlsruhe.

Method

The magnetic field contribution of the coils is calculated as described previously[3] using the law of Biot and Savart. To compute the iron contribution we use an integral method which does not need a mesh outside the iron. The torus is enclosed in a regular array of curved volume elements with rectangular cross-section (Fig. 2). Each element contains a segment of the torus or part of it whose volume and center of gravity can be calculated analytically thanks to this particular discretization. The magnetization of each element is represented by a magnetic

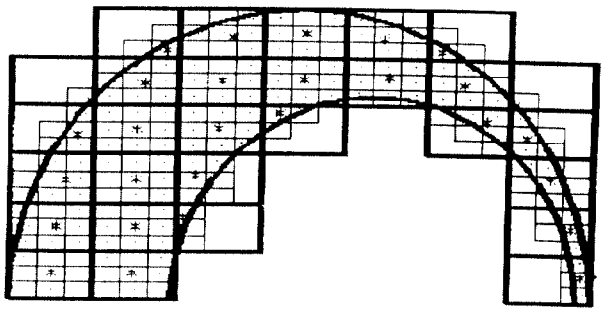

Fig. 2: Discretization of the torus for the first iteration step.

dipole located in the center of gravity. The size of the elements is controlled dynamically: if, for instance, the center of gravity of a neighbouring element comes closer to the element under consideration than 5 times the element size, this element is divided into 27 subelements. If the other element is closer than 3 times the original element size, the element under consideration is divided into 1000 parts. For the self-contribution of the elements we use a similar method combined with analytic formulae of the magnetic coefficients as given in ref. 4.

In this way, we get the coefficients of the Fredholm equation of the second kind which we solve in two steps: first, we start with a crude mesh (typically 200 elements for a quarter of the 90° bending magnet) using a direct method with Gaussian elimination and a Newton-Raphson iteration updating the permeability at each step. Then, the magnetization values are distributed in a finer mesh (typically 1400 cells) as starting values for a Gauss-Seidel iteration. Fig. 2 illustrates the initial mesh and its first subdivisions (27 in volume, 9 in a plane).

From the magnetic field data the coefficients of the transfer map in the Lie algebraic formalism are computed by means of the code NIN/SCB[5]. This code gives the 3rd order map for the magnet referred to the real design orbit in a form suitable for use with MARYLIE[6] to do a symplectic nonisomagnetic 3rd order tracking of the particles. The tracking subroutine in MARYLIE has been extended to allow an iterative determination of the stability limit of a trajectory.

Results and discussion

Bending magnet

The bending magnet is built up of several coils distributed over two layers each 1 cm thick having circular cross-section. The coils are surrounded by a C-shaped iron shield. The inner and outer radius of the coil layers are 6 cm and 8 cm, respectively. The iron shield has an inner radius of 14 cm and a maximum thickness of 11 cm. In the longitudinal direction, the coil and the iron shield extend over an angular range

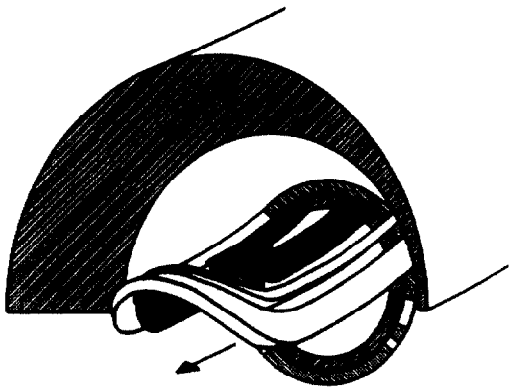

Fig. 3: 3D view of the end of the bending magnet.

of 90° and 30°, respectively. Fig. 3 gives a 3D view of the end of the magnet. In contrast to a previously described air coil[7], the present coil has no quadrupole winding to compensate the gradient caused by the curvature. Instead, the iron shield produces a gradient itself which nearly compensates the curvature gradient.

Magnetic field

Fig. 4 shows the transverse relative field deviation for the three field cases and for two iron shields differing by the inner radius. The maximum contribution of the iron shield, in the case of the inner radius being 14 cm, is 0.429 T at 4 T integral field strength, 0.0699 T at 0.4 T, and 0.1538 T at 1.0 T from which nonlinear behaviour of the field can be seen.

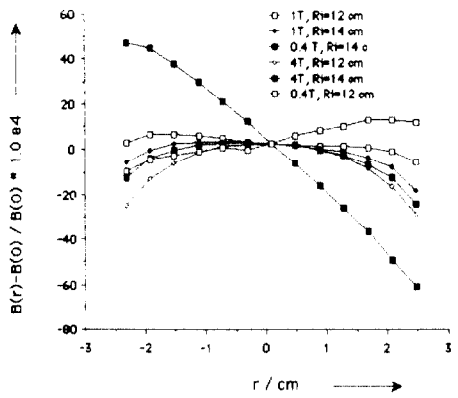

Fig. 4: Relative field deviation in the center of the magnet for the two inner radii of iron of 12 and 14 cm.

The main differences in field behaviour along the electron orbit are found in the coil end region. Fig. 5 gives the longitudinal dependence of the vertical field component normalized to its value on axis in the center of the magnet. The negative field overshoot arising from the coil return is reduced at lower field strength due to the larger relative contribution to the field from the iron shield.

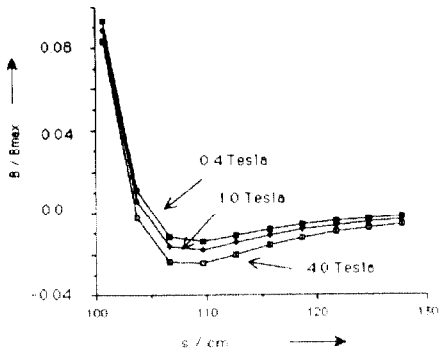

Fig. 5: Field along the reference orbit in the end region. The inner radius of the iron is 14 cm. s = 0 corresponds to the center of the magnet.

Dynamic aperture

Fig. 6 shows the dynamic aperture for the three field cases. The larger apertures hold for the case that the chromaticity is not compensated. The influence of the field strength is not very pronounced.

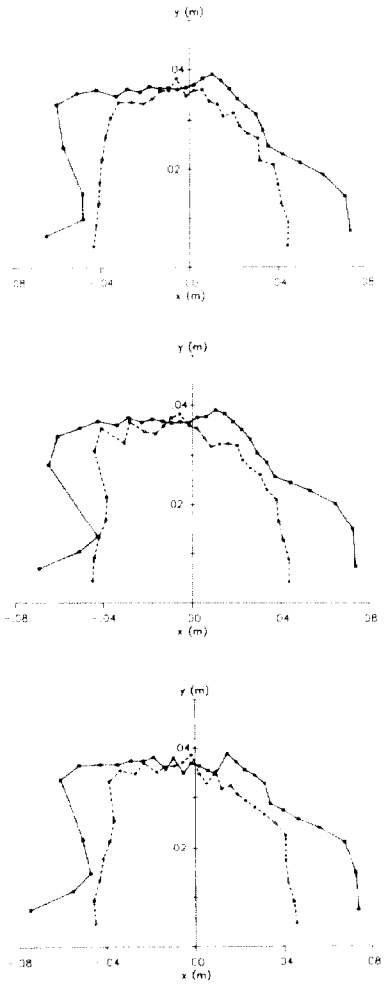

Fig. 6: Dynamic apertures for the field levels 4.0, 1.0, and 0.4 T with (dashed line, circles) and without (solid line, squares) chromaticity compensating sextupoles. Inner radius of iron shield is 14 cm.

However, there are regions, at large horizontal amplitudes, where the dynamic aperture gets larger with decreasing field which might point to a favourable influence of the iron. The smaller apertures are obtained when the chromaticity is set to about 0.1 for both planes by means of sextupoles. It can be seen that the variation of the dynamic apertures as function of the field strength is much smaller than the influence of the sextupoles . Fig. 7 displays dynamic apertures for a different inner radius of the iron shield in the 4 T and 1 T cases. It can be seen that the dynamic aperture gets larger when the iron shield is closer, at constant field, and when the field is smaller, at fixed iron geometry. On the basis of these calculations, the dynamic aperture becomes larger with increasing relative contribution of the iron shield. In all cases, the dynamic aperture is large enough to achieve a satisfactory beam lifetime.

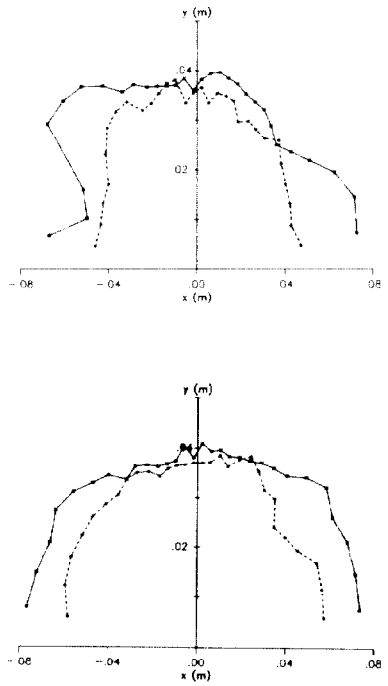

Fig. 7: Dynamic apertures for the field levels 4.0 and 1.0 T with (dashed line, circles) and without (solid line, squares) chromaticity compensating sextupoles. Inner racius of iron shield is 12 cm

Conclusion

Magnetic field calculations for the case of a 90° bencing magnet with superconducting coils of cylindrical cross-section surrounded by an iron shield show nonlinear variations of the field depending on the integral field strength. The dynamic apertures obtained from symplectic nonisomagnetic 3rd order tracking show a tendency to become larger with increasing relative contribution of the iron to the field.

References

[1] see, e.g., G. Dugan, "The Tevatron: Status and Outlook", in EPAC 88, S. Tazzari, ed., World Scientific, Singapore, 1988, pp. 223-227; T. Hosokawa et al., "NTT Superconducting Storage Ring - Super-ALIS", Rev. Sci. Instrum. , vol. 60, pp. 1783-1785, 1989; H Yamada, T. Takayama, and T. Hori, "Operation Experiences of AURORA: The Compact Synchrotron Light Source", this conference.

[2] D. Einfeld et al., "Entwurf einer Synchrotronstranlungsquelle mit supraleitenden Ablenkmagneten für die Mikrofertigung nach dem LIGA-Verfahren", Kernforschungszentrum Karlsruhe, Report KfK 3976, September 1985.

[3] B. Krevet, H.O. Moser, C. Dustmann, "Design of a Strongly Curved Superconducting Bending Magnet for a Compact Synchrotron Light Source", in Advances in Cryogenic Engineering, vol. 33, R.W. Fast, ed., Plenum Press, New York, 1988.

[4] L.R. Turner, "Direct Calculation of Magnetic Field in the Presence of Iron, as applied to the Computer Program GFUN", Rutherford Laboratory, RL-73-102, 1972.

[5] H.O. Moser, A.J. Dragt, "Influence of Strongly Curved Large-Bore Superconducting Bending Magnets on the Optics of Storage Rings", Nucl. Instr. and Meth., vol. B24/25, pp. 877-879, 1987.

[6] A.J. Dragt et al., "MARYLIE 3.0: A Program for Charged Particle Beam Transport Based on Lie Algebraic Methods", University of Maryland, College Park, MD 20742, 1985.

[7] H.O. Moser, B. Krevet, "Emittance and Dynamic Aperture in Compact Storage Rings with Superconducting Bending Magnets", in EPAC 88, S. Tazzari, ed., World Scientific, Singapore, 1988, pp. 794-796.